Front Surface Grid Design for High Efficiency Solar Cells

Utpal Gangopadhyay, Kyunghae Kim, Prabir Kanti Basu, Suresh Kumar Dhungel, Sungwook Jung, and Junsin Yi[a]
School of Electrical and Computer Engineering, Sungkyunkwan University, Cheoncheon-dong, Jangan-gu, Suwon-si, Kyunggi 440-746, Korea

Swapan Kumar Dutta and Hiranmoy Saha
Department of Electronics and Tele-communication Engineering, Jadavpur University, Calcutta, 700032, INDIA

[a]E-mail : yi@yurim.skku.ac.kr

(Received October 25 2004, Accepted April 14 2005)

Standard crystalline solar cells are generally fabricated with the front grid pattern of silver paste contact. We have reported a detailed theoretical analysis of the proposed segmented cross grid line pattern in this paper. This work was carried out for the optimization of spacing and width of grid finger, main busbar and sub-busbar. The overall electrical and optical losses due to front contact were brought down to 10 % or even less as compared to the usual loss of 15 % or more in the conventional screen printed silver paste technology by choosing proper grid pattern and optimizing the grid parameters. The total normalized power loss for segmented mesh grid with plated metal contact was also observed and the total power loss could be brought down to 10.04 % unlike 11.57 % in the case of continuous grid and plated contact. This paper is able to outline the limitations of conventional screen printed contact.

Keywords : Solar cell, High efficiency, Grid, Metallization

1. INTRODUCTION

A solar cell is a photodiode which is used to convert light energy to electrical energy and it thereby serves as a source of d.c. power under illumination. Usually, a solar cell (e.g. silicon solar cell) consists of a thick p-layer (base) with a thin n-layer (emitter) on top of it forming a shallow p-n junction. Light penetrates through the emitter layer (the front surface) to the base, generates excess minority carriers which is made to flow through a load via the metal contacts to the front and back surface of the cell. Having a close look at the front surface, we can easily see from Fig. 1 that the two dominating sources of loss in cell efficiency[1,2] are

i) the shadowing or optical loss due to the coverage of a part of the surface by metal contact lines and
ii) the resistive losses due to carrier flow in the emitter layer, semiconductor-metal contact and in the metal contact lines.

If we cover the front surface of the entire cell with a metal layer, the optical loss will be maximum and the resistive loss will be minimum. On the other hand, if no contacts are made to the front surface, the incident light can be totally utilized so that the optical loss is minimum, but no power can be taken out of the solar cell. Therefore the front surface metal contact pattern is decided by two contradictory criteria,

a) Minimizing the electrical/resistive losses by increasing the width of the contact lines.
b) Minimizing the optical losses by decreasing the width of the contact lines.

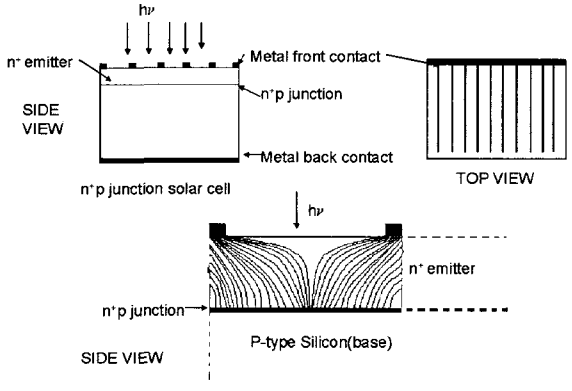

Fig. 1. Schematic diagram of the current flow through the emitter to the two consecutive metal strips on the front surface of a solar cell.

The electrical losses also depend on the specific sheet resistance of the metal contact lines of the emitter layer. Therefore, the geometry of the metal contact lines (called the grid pattern) is very important from the point of view of minimization of loses.

In optimum grid geometry, a compromise must be arrived at between the surface area coverage of the grid and its associated resistive loss incurring a maximum total loss.

2. THEORY

Figure 2 shows a few typical front surface grid contact patterns. Two types of metal lines can be identified namely (a) busbar and (b) fingers. Busbars are relatively thick areas of metallization from which direct external connections are taken while the fingers are finer elements which collect current for delivery to the busbar.

The grid contact may also consist of more than a single busbar and consequently more than one set of fingers. Also, fingers and busbars may be of constant width, linearly tapered or have step changes in width. The different front contact designs are made keeping principally in view of the shape and size of the front surface, the specific sheet resistances of the emitter layer and metal used and also the electrical parameters (J_{mp}, V_{mp}) of the cell. However, as we shall see that in many cases, the actual grid pattern may be dictated by the limitations of the technical process through which the grid metallization schemes are realized in practice.

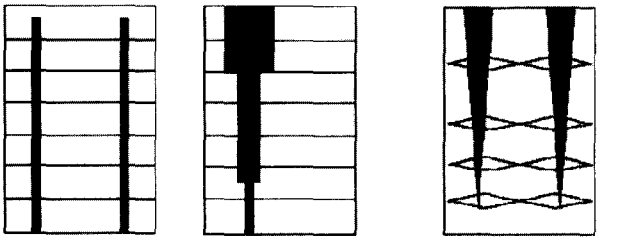

Fig. 2. Different front contact grid pattern.

2.1 Analysis of losses in the metal grid contact

A symmetrical grid pattern scheme consisting of two uniform busbars and equally spaced uniform fingers is shown in Fig. 3. The maximum power output that can be drawn from the cell is J_{mp}, V_{mp} AB where AB is the area of the cell. J_{mp} and V_{mp} are current density and voltage at the maximum power point respectively.

The electrical & optical power losses normalized to the maximum output of the cell (fractional losses) can be calculated to give the following results

A. Resistive power losses

a) Fractional resistive power loss due to lateral current flow in the emitter layer

$$p_{t1} = \frac{1}{12}\rho_s s^2 \left(\frac{J_{mp}}{V_{mp}}\right) \tag{1}$$

where ρ_s = Sheet resistivity of the emitter layer $= \frac{\rho_{silicon}}{t}$, [$\rho_{silicon}$ = Resistivity of silicon emitter layer and t=thickness of emitter layer] and S=pitch of the fingers

b) Fractional resistive power loss in the fingers

$$p_{rf} = \frac{1}{3}\rho_{smf}\left(\frac{S}{W_f}\right)b_1^2\left(\frac{J_{mp}}{V_{mp}}\right)$$

$$= \frac{1}{3}\rho_{smf}\left(\frac{S}{W_f}\right)\left(\frac{B/2 - W_b}{2}\right)^2\left(\frac{J_{mp}}{V_{mp}}\right) \tag{2}$$

where b_1=length of each current collecting finger on either side of the busbar and W_b=Width of busbar.

c) Fractional resistive power loss due to contact resistance

$$p_{cf} = \rho_c\left(\frac{S}{W_f}\right)\left(\frac{J_{mp}}{V_{mp}}\right) \tag{3}$$

where ρ_c = Specific contact resistance of the metal with the semiconductor (Silicon).

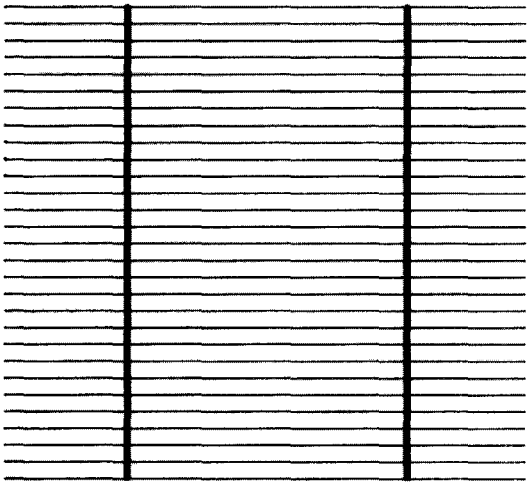

Fig. 3. Continuous finger front grid pattern.

d) Fractional resistive power loss in the busbars

$$p_{rb} = \frac{2}{3} A^2 b_l \left(\frac{\rho_{smb}}{W_b} \right) \left(\frac{J_{mp}}{V_{mp}} \right) \quad (4)$$

where ρ_{smb} = Sheet resistivity of the busbars

B. Optical power losses

a) Fractional optical power loss in the fingers

$$p_{sf} = \frac{W_f}{S} \quad (5)$$

b) Fractional optical power loss in the busbars

$$p_{sb} = \frac{W_b}{(B/2)} \approx \frac{W_b}{2b_l} \quad (6)$$

The total fractional power loss will then be given by

$$p = p_{res} + p_{opt} = (p_{tl} + p_{rf} + p_{rb}) + (p_{sf} + p_{sb}) \quad (7)$$

It can be easily seen that except p_{rb} and p_{sb}, other losses do not have any dependence on W_b. Therefore, the losses in the busbar can be optimized independently and it occurs when the optical loss in the busbar equals its resistive loss and the optimized W_b is given by

$$W_b = 2Ab_l \sqrt{\left[\frac{1}{3} \rho_{smb} \left(\frac{J_{mp}}{V_{mp}} \right) \right]} \quad (8)$$

The optimization of finger spacing (S) and finger width (W_f) will be more complex. The optimization will occur when $S \rightarrow 0$

and simultaneously

$$\frac{W_f}{S} = \sqrt{\left[\left(\frac{1}{3} \rho_{smf} b_l^2 + \rho_c \right) \left(\frac{J_{mp}}{V_{mp}} \right) \right]} \quad (9)$$

with these considerations, we can calculate the optimum values of W_b, W_f and S for optimum performance of the cells. However, it can be seen easily that lower and lower S and simultaneously lower value of W_f will produce lower losses.

However, each of the grid formation technologies has its limitation on how small W_f and S can be made and therefore the adopted technology sets the limit for minimum losses.

Therefore, we will now calculate numerically the losses for the screen printed silver contacts which are mostly used for commercial silicon solar cells.

2.1.1 Numerical calculations for screen printed silver contacts

The contact pattern is formed by printing silver paste through the openings in a screen on to the wafer. A good electrical and mechanical contact is obtained after drying and firing using conventional conveyor belt furnace[3]. In this technique, it is generally difficult to go below 100 μm wide finger lines and this sets the technological limit towards optimization of grid design.

The calculations are based on the following input data:-

i) Sheet resistivity of Silver : $\rho_{smf}=3.57\times10^{-3}$ Ω/□ (On the finger lines)

ii) Width of Silver layer = 100 μm

iii) Sheet resistivity of busbar : $\rho_{smb}=1.88\times10^{-3}$ Ω/□ (Silver + 80 μm solder layer on top)

iv) Specific contact resistance : $\rho_c=0.37\times10^{-3}$ Ω.cm^2

v) Sheet resistivity of silicon n^+ emitter layer : ρ_s=30 Ω/□

vi) Electrical parameters : J_{mp}=30 mA/cm^2
V_{mp}=0.48 Volts.

vii) Cell geometry : 10 cm × 10 cm pseudo - Square

viii) Finger width : 100 μm

From the calculation with the help of a computer program, we get,

Optimized Width of Busbar = 2940 μm

Optimized Finger Spacing ≈ 2.8 mm.

p_{cf} = 0.06 % ; p_{tl} = 1.23 % ; p_{rf} = 1.09 %; p_{rb} = 6.26 %

T_{EL} =Total Electrical loss = 8.64 %

also p_{sf} = 3.57 ; p_{sb} = 6.25

So, T_{OL} = Total optical loss = 9.82 %

Total power loss = TL = T_{EL} + T_{OL} = 18.46 %

It can be seen from the above calculations that the major contribution towards the total loss comes from resistivity & shadowing loss of busbars. This is due to the fact that silver resistivity is high so that the larger width of the busbar has to be taken.

Further, the silver contact has the following disadvantages:-

i) Little control on the thickness of the deposited silver.

ii) Expensive material (~40 % cost of a solar cell comes from the metallization).

iii) Lower resolution of grid pattern.

iv) Considerable wastage of material.

Therefore, one should look forward to other technological process to overcome these difficulties.

This can be done by employing electroless and electroplated contacts and also using the novel negative screen technology.

In this method, a negative screen is printed on the wafer where the wafer is covered with ink except the grid contact lines. Then the grid contact is formed by

successive plating of nickel (Ni) and copper and soldered in the following manner.

3. EXPERIMENTAL OF PLATED METALLIZATION PROCESS

a) Electroless deposition of Nickel : In this method, first 100 mm×100 mm wafers were textured by conventional NaOH bath[4] followed by $POCl_3$ diffusion and wet edge isolation[5,6]. Then all edge isolated diffused samples were first masked with the help of screen printed ink followed by baking in a conventional conveyor belt furnace. They were then treated with an etchant (p-etch) for few seconds, rinsed with DI water & then placed in a nickel solution bath maintained at around 70 °C[7]. The samples, dipped in the bath for about 20 min were then taken out and again rinsed with DI water. Nickel was found to be deposited on the etched grid lines and rear surface of solar cells. The deposited Ni was around 2 micron thick.

b) Electrochemical deposition of Copper : Copper was electrochemically deposited over the Ni layer by dipping the samples in a copper sulphate solution. A potentiostat was used to supply a constant voltage around 300 ㎷ to the sample against a reference electrode, the counter electrode being a graphite rod. A deposition time of about 1 hour yielded a copper thickness of nearly 70-80 microns.

c) Electrochemical deposition of Solder : Two solutions were used for this deposition.

(i) The standard fluoborate solution of tin and lead and (ii) An acetate solution of tin and lead developed by us. The constituents of the electrosolder solutions are as follows:

Boric acid=2.5 gm / 2 litre.
Gelatin=0.064 gm / 2 litre.
Resorcinol=0.064 gm / 2 litre.
Fluboric acid=10 gm / 2 litre.
Tin Fluborate=27.50 gm / 2 litre.
Lead Fluborate=49.92 gm / 2 litre.

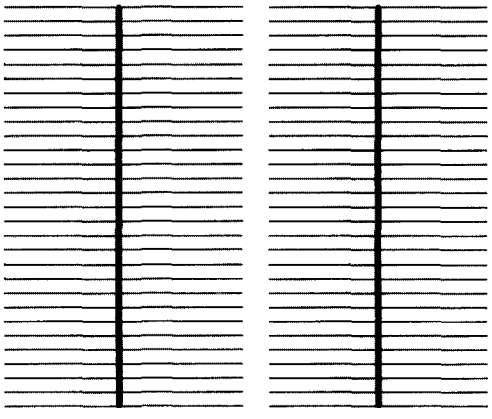

Fig. 4. Segmented front grid finger pattern.

The solder was electrochemically deposited on top of copper similarly as above, with a constant voltage of about 500 ㎷. A thickness of 9-10 ㎛ could be achieved for 30 mins deposition.

Using these plated metallization, the following three types of grid pattern have been considered.

a) Continuous grid (Fig. 3)
b) Segmented grid (Fig. 4)
c) Segmented mesh grid (Fig. 5 and Fig. 6)

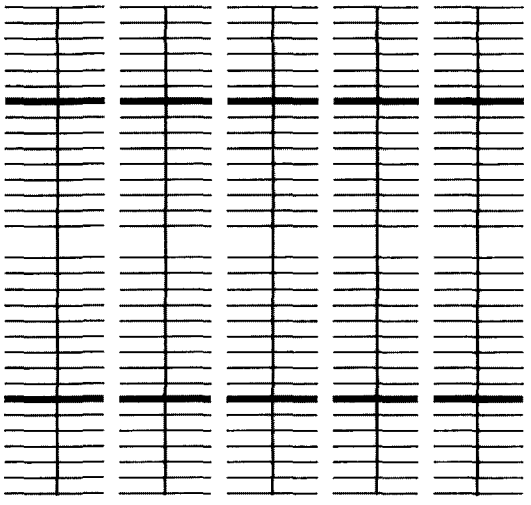

Fig. 5. Segmented mesh front grid pattern with uniform busbars.

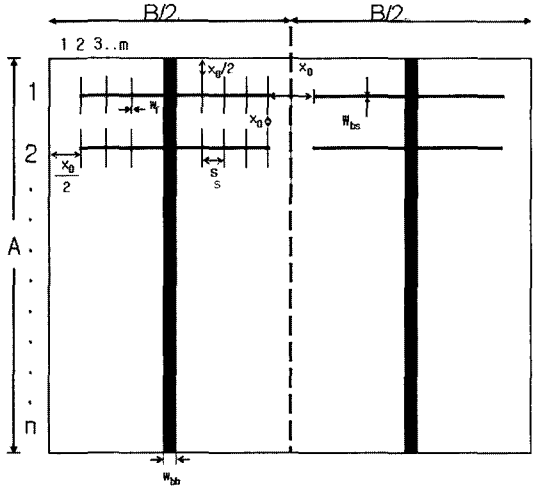

Fig. 6. Different geometrical parameters for segmented mesh grid.

3.1 Analysis and calculation with plated metal grid contacts

The fractional electrical and optical power losses in each of these proposed grid pattern have been theoretically analyzed and computed numerically using a

specially developed computer program.

The analytical expressions for the segmented grid structure and segmented mesh grid structure are as follows:

A. Segmented grid

a) Resistive fractional power loss in the emitter layer

$$p_{t1} = \frac{1}{12}\rho_s s^2 \left(\frac{J_{mp}}{V_{mp}}\right) c_1 \tag{10}$$

where ρ_s = Sheet resistivity of the emitter layer $= \frac{\rho_{silicon}}{t}$,

and $c_1 = \left[\left(\frac{1+\frac{x_o}{6b}\left(1+\frac{x_o^2}{s^2}\right)}{1+\frac{x_o}{2b}}\right)\right]$

b) Fractional resistive power loss in the fingers

$$p_{rf} = \frac{1}{3}\rho_{smf}\left(\frac{S}{W_f}\right) b_1^2 \left(\frac{J_{mp}}{V_{mp}}\right) c_2 \tag{11}$$

$$= \frac{1}{3}\rho_{smf}\left(\frac{S}{W_f}\right)\left(\frac{B/2 - W_b}{2}\right)^2 \left(\frac{J_{mp}}{V_{mp}}\right) c_2$$

where b_1 = length of each current collecting finger on either side of the busbar

W_b = Width of busbar,

and $c_2 = \left[\left(\frac{1+\frac{3x_o}{2b}+\frac{3x_o^2}{4b^2}}{1+\frac{x_o}{2b}}\right)\right]$

c) Fractional resistive power loss due to contact resistance

$$p_{cf} = \rho_c \left(\frac{S}{W_f}\right)\left(\frac{J_{mp}}{V_{mp}}\right) c_3 \tag{12}$$

where ρ_c = Specific contact resistance of the metal with the semiconductor (silicon).

and $c_3 = \frac{1}{1+\frac{x_o}{2b}}$

d) Fractional resistive power loss in the busbars

$$p_{rb} = \frac{2}{3}A^2 b_1 \left(\frac{\rho_{smb}}{W_b}\right)\left(\frac{J_{mp}}{V_{mp}}\right) c_3 \tag{13}$$

where ρ_{smb} = Sheet resistivity of the busbars.

B. Optical power losses

a) Fractional optical power loss in the fingers

$$p_{sf} = \frac{W_f}{S} c_3 \tag{14}$$

b) Fractional optical power loss in the busbars

$$p_{sb} = \frac{W_b}{(B/2)} \approx \frac{W_b}{2b_1} c_3 \tag{15}$$

C. Segmented mesh grid

a) Resistive fractional power loss in the emitter layer

$$p_{ti} = \frac{1}{12}\rho_s S^2 \left(\frac{J_{mp}}{V_{mp}}\right) c_1 \tag{16}$$

b) Fractional resistive power loss in the fingers

$$p_{rf} = \frac{1}{3}\rho_{smf}\left(\frac{S}{W_f}\right) l_b^2 \left(\frac{J_{mp}}{V_{mp}}\right) c_2 \tag{17}$$

where $l_b = \left(\frac{\frac{B}{2} - X_o - W_{b2}}{2}\right)$

c) Fractional resistive power loss due to contact resistance

$$p_{cf} = \rho_c \left(\frac{S}{W_f}\right)\left(\frac{J_{mp}}{V_{mp}}\right) c_3 \tag{18}$$

where ρ_c = Specific contact resistance of the metal with the semiconductor (silicon)

d) Fractional resistive power loss in the small busbars

$$p_{rb1} = \frac{2}{3} b l_b^2 \left(\frac{\rho_{smb1}}{W_{b1}}\right)\left(\frac{J_{mp}}{V_{mp}}\right) c_3 \tag{19}$$

where ρ_{smb1} = Sheet resistivity of the small busbars.

e) Fractional resistive power loss in the big busbars

$$p_{rb2} = \frac{2}{3} A^2 l_b \left(\frac{\rho_{smb2}}{W_{b2}} \right) \left(\frac{J_{mp}}{V_{mp}} \right) c_3 \qquad (20)$$

where ρ_{smb2} = Sheet resistivity of the big busbars.

Optical power losses:

a) Fractional optical power loss in the finger

$$p_{sf} = \left(\frac{W_f}{S} \right) c_3 \qquad (21)$$

b) Fractional optical power loss in the small busbars

$$p_{sb1} = \left(\frac{W_{b1}}{2b} \right) c_3 \qquad (22)$$

c) Fractional optical power loss in the big busbars

$$p_{sb2} = \left(\frac{W_{b2}}{2l_b} \right) c_3 \qquad (23)$$

where $c_1 = \left[\left(\frac{1 + \frac{x_o}{6b}\left(1 + x_o^2 / s^2\right)}{1 + \frac{x_o}{2b}} \right) \right]$

$$c_2 = \left[\left(\frac{1 + \frac{3x_o}{2b} + \frac{3x_o^2}{4b^2}}{1 + \frac{x_o}{2b}} \right) \right]$$

$$c_3 = \frac{1}{1 + \frac{x_o}{2b}}$$

Following inputs are used for numerical calculations:

i) Solar cell geometry=100 mm×100 mm pseudo square

ii) Electrical parameters : J_{mp}=30 mA/cm^2
V_{mp}=0.48 V

iii)The resistive losses due to carrier flow in the emitter layer, semiconductor-metal contact and in the metal contact lines.

iv) Sheet resistivity of emitter layer=ρ_s=30 Ω/□

v) Sheet resistivity of the finger and small busbars multi-layer metals=0.228 mΩ/□

vi) Sheet resistivity of the big busbar soldered with interconnecting strip=0.083 mΩ/□

vii) Specific contact resistance of the metal layers with silicon=16.7 mΩ/cm^2

The calculations have also been done by talking big busbar width in steps. It can be shown that if $(W_{b2})_{opt}$ is the optimum width for uniform big busbar, then the starting width of the busbar in steps will be given by

$$N(W_{b2})_{opt} = \sqrt{3}\left[(W_{b2})_{opt}\right] \qquad (24)$$

where N=number of small busbars.

Table 1 shows the geometrical dimensions of the grid pattern viz. widths of the grid finger lines(W_f), small (W_{b1}), big(W_{b1}) busbars, separation between finger segments(X_o) etc. for optimized minimum total loss.

Table 1. Normalized power losses for optimized grid patterns of different type.

Type of grid pattern	Parameters used	Total normalized optical loss (%)	Total normalized electrical power loss (%)	Total normalized power loss (%)
Continuous finger	S=2.40 mm W_f=100 μm W_b=640 μm	5.46	6.10	11.57
Segmented grid Finger	S=2.4 mm W_f=100 μm W_b=640 μm X_o = 5 mm	5.21	5.94	11.15
Segmented grid finger with uniform big busbar	S=2.4 mm W_f=100 μm W_{bs}=100 μm W_{bb}=670 μm X_o =5 mm N=5	5.11	4.93	10.04

It may be pointed out that the minimum finger width has been taken to be 100 μm since it is understood that it may not be possible to realize lower widths with the available screen printed technology. With the improvement of screen printing technology, it is expected that grid finger width as low as 30-50 μm, using plated technology, can be realized.

4. RESULTS AND DISCUSSION

It is evident from table 1 that the optimized total losses in all the three grid patterns are only marginally different. The selection of the grid pattern is therefore dictated by the technology to be used for grid formation. If standard silver paste screen printing processing is to be used, the continuous grid finger pattern is alright. However, for plating processing, as the metal is deposited inside the narrow channels, the possibility of having discontinuities increases with increasing length of narrow finger lines. This is why a segmented mesh grid pattern is more compatible to plating processes. Further with plating process, the thickness of the grid fingers and busbars can be increased to the desired value in order to attain lower sheet resistivity of the grid fingers and busbars so that narrower fingers could be used for the same specified electrical loss while the optical loss will decrease further with increasing separation between the segments of the grid finger. The sheet resistance of the diffused layer can also be optimized for the separation between the grid segments.

5. CONCLUSION

The different grid structure based on plated metal contact on silicon solar cells have been analyzed in details. The segmented grid mesh structure with uniform big busbars and small busbars in steps are found to be attractive from the point of view of both technical and theoretical considerations.

REFERENCES

[1] M. A. Green, "Solar Cells – Operating Principles and Technology and System Application", UNSW, p. 153, 1982.

[2] M. F. Stuckings and A. W. Blankers, "A study of shading and resistive loss from fingers of encapsulated solar cells", Solar Energy Materials and Solar Cells, Vol. 59, No. 3, p. 233, 1999.

[3] W. Neu, A. Kress, W. Jooss, P. Fath, and E. Bucher, "Low cost multicrystalline back contact silicon solar cells with screen printed metallization", Solar Energy Materials and Solar Cells, Vol. 74, No. 1-4, p. 139, 2002.

[4] E. Vazsonyi, K. D. Clercq, R. Einhaus, E. Van Kerschaver, K. Said, J. Poortmans, J. Szlufcik, and J. Nijs, "Improved anisotropic etching process for industrial texturing of silicon solar cells", Solar Energy Materials and Solar Cells, Vol. 57, No. 2, p. 179, 1999.

[5] S. Bourdias, G. Beaucarne, A. Slaoui, J. Poortmans, B. Semmache, and C. Dubois, "Comparative study of rapid and classical thermal phosphorus diffusion on polycrystalline silicon thin films", Solar Energy Materials and Solar Cells, Vol. 65, No. 1-4, p. 487, 2001.

[6] S. Bandopadhyay, U. Gangopadhyay, K. Mukhopadhyay, H. Saha, and A. P. Chatterjee, "Nickel silicide contact for silicon solar cells", Bull. Mater. Sci., Vol. 15, No. 5, p. 473 , 1992.

[7] U. Gangopadhyay, K. Sinha, and H. Saha, "Auto-catalytic nickel plating on different silicon surface", Indian J. Phys., Vol. 61A, p. 266, 1987.